Dimensionality of superconductivity in the infinite-layer high-temperature cuprate $Sr_{0.9}M_{0.1}CuO_2$ (M = La, Gd)

V. S. Zapf,[1] N.-C. Yeh,[1] A. D. Beyer,[1] C. R. Hughes,[1] C. H. Mielke,[2] N. Harrison,[2] M. S. Park,[3] K. H. Kim,[3] S.-I. Lee,[3]
[1]*Department of Physics, California Institute of Technology, Pasadena, CA*
[2]*National High Magnetic Field Laboratory, Los Alamos, NM*
[3]*Department of Physics, Pohang University of Science and Technology, Pohang, Korea*
(Dated: October 20, 2004)

The high magnetic field phase diagram of the electron-doped infinite layer high-temperature superconducting (high-T_c) compound $Sr_{0.9}La_{0.1}CuO_2$ was probed by means of penetration depth and magnetization measurements in pulsed fields to 60 T. An anisotropy ratio of 8 was detected for the upper critical fields with H parallel (H_{c2}^{ab}) and perpendicular (H_{c2}^{c}) to the CuO_2 planes, with H_{c2}^{ab} extrapolating to near the Pauli paramagnetic limit of 160 T. The longer superconducting coherence length than the lattice constant along the c-axis indicates that the orbital degrees of freedom of the pairing wavefunction are three dimensional. By contrast, low-field magnetization and specific heat measurements of $Sr_{0.9}Gd_{0.1}CuO_2$ indicate a coexistence of bulk s-wave superconductivity with large moment Gd paramagnetism close to the CuO_2 planes, suggesting a strong confinement of the spin degrees of freedom of the Cooper pair to the CuO_2 planes. The region between H_{c2}^{ab} and the irreversibility line in the magnetization, $H_{\rm irr}^{ab}$, is anomalously large for an electron-doped high-T_c cuprate, suggesting the existence of additional quantum fluctuations perhaps due to a competing spin-density wave order.

PACS numbers: 74.25.Dw,74.25.Op,74.72,Dn,74,25.Bt,74.25.Fy,74.25.Ha
Keywords: cuprate, superconductivity, infinite layer, competing order, upper critical field, Gd substitution

In the high-T_c cuprate superconductors, anisotropy has been suggested to play an important role in the superconducting pairing mechanism and the elevated T_c in both experimental and theoretical work [1, 2]. It is surprising therefore to find superconductivity (SC) with T_c = 43 K in the optimal electron-doped infinite-layer cuprates $Sr_{0.9}M_{0.1}CuO_2$ (M = La, Gd), which exhibit only a 16% difference between the a and c tetragonal lattice parameters. The structure of $Sr_{0.9}M_{0.1}CuO_2$ is the most basic among all high-T_c cuprates, consisting entirely of CuO_2 sheets separated by rare-earth (RE) ions with tetragonal lattice parameters c = 3.41 Å and a = 3.95 Å.[3] The recent success in producing high-quality polycrystalline samples of the infinite-layer cuprates with no observable impurity phases [3] has engendered a renewed interest in these compounds. X-ray near-edge absorption spectroscopy indicate electron doping, [4] and bulk SC has been verified by powdered magnetization (M) measurements [5] and specific heat (C) measurements (data presented later in this work). Several recent studies of these high purity polycrystalline samples suggest three-dimensional (3D) superconductivity in $Sr_{0.9}La_{0.1}CuO_2$. Scanning tunnel spectroscopy (STS) measurements [6] indicate an unconventional but isotropic s-wave superconducting gap with no pseudogap at zero field. The s-wave symmetry of the gap is also supported by specific heat measurements and Cu-site substitution studies,[6, 7, 8] although it may be contradicted by NMR measurements.[9] Kim et al [5] estimated the c-axis coherence length (ξ_c) from a Hao-Clem analysis [10] of the reversible magnetization of grain-aligned polycrystal, and found that ξ_c exceeds the spacing between the CuO_2 planes, indicating 3D superconductivity. On the other hand, they also find significant anisotropy between magnetic fields $H \leq 5$ T oriented parallel and perpendicular to the CuO_2 planes, with an anisotropy ratio $\gamma = \xi_c/\xi_{ab} = H_{c2}^{ab}/H_{c2}^{c} = 9.3$, which is larger than $\gamma = 5$ observed in $YBa_2Cu_3O_{7-\delta}$ although much smaller than $\gamma = 55$ observed in optimally doped $Bi_2Sr_2CaCu_2O_{8-\delta}$. [5, 11, 12, 13] It is interesting to note that the only major crystallographic difference between the a-b and the c directions in $Sr_{0.9}La_{0.1}CuO_2$ is the presence of oxygen in the a-b plane, which allows coupling of adjacent Cu spins and has been implicated as the cause of antiferromagntic ordering or spin fluctuations in other members of the high-T_c cuprate family, as well as a possible mechanism for superconducting pairing. The importance of the CuO_2 planes to the SC in $Sr_{0.9}M_{0.1}CuO_2$ is further supported by the fact that Ni substitution on the Cu site rapidly suppresses T_c whereas out-of-plane Gd substitution on the Sr site leaves T_c unchanged. [7, 14]

In this work we determine the upper critical field H_{c2} and the irreversibility field $H_{\rm irr}$ of $Sr_{0.9}La_{0.1}CuO_2$ by means of magnetization and penetration depth measurements in pulsed magnetic fields up to 60 T in order to directly investigate the degree of upper critical field anisotropy and the role of vortex fluctuations. We also present specific heat (C) and magnetization (M) measurements in low DC fields to 6 T as a function of temperature (T) of $Sr_{0.9}Gd_{0.1}CuO_2$, confirming the bulk coexistence of Gd paramagnetism (PM) and SC. Our results suggest strong confinement of the spin pairing wave function to the CuO_2 planes and significant field-induced superconducting fluctuations.

Noncrystalline samples of $Sr_{0.9}La_{0.1}CuO_2$ and $Sr_{0.9}Gd_{0.1}CuO_2$ were prepared under high pressures as described previously. [3] Magnetization measurements in pulsed magnetic fields were performed at the National

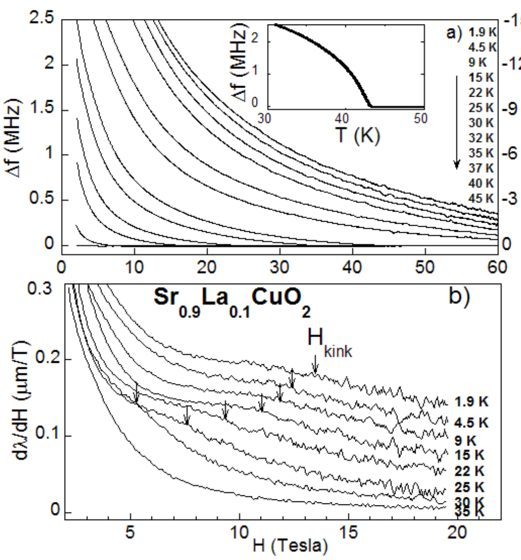

FIG. 1: a) Change in resonant frequency Δf of the TDO tank circuit relative to the normal state of $Sr_{0.9}La_{0.1}CuO_2$ as a function of magnetic field H of $Sr_{0.9}La_{0.1}CuO_2$ polycrystal at various temperatures T. The estimated change in penetration depth λ is indicated on the right axis. Inset: Δf as a function of T at zero field where $T_c = 43K$. b) Derivative of λ with H for various T, with arrows indicating $H_{\rm kink}$.

High Magnetic Field Laboratory (NHMFL) in Los Alamos, NM in a ^{3}He refrigerator in a 50 T magnet using a compensated coil. The sample consisted of four pieces of polycrystalline $Sr_{0.9}La_{0.1}CuO_2$ with a total mass of 4.8 mg to maximize signal and minimize heating. The irreversibility field $H_{\rm irr}$ was identified from the onset of reversibility in the $M(H)$ loops. The penetration depth of $Sr_{0.9}La_{0.1}CuO_2$ was determined by measuring the frequency shift Δf of a tunnel diode oscillator (TDO) resonant tank circuit with the sample contained in one of the component inductors. [15] A ten turn 0.7 mm diameter aluminum coil was tightly wound around the sample with a filling factor of greater than 90%, with the coil axis oriented perpendicular to the pulsed field. To maintain temperature stability, the sample was thermally anchored to a sapphire plate and placed in ^{3}He exchange gas. Small changes in the resonant frequency can be related to changes in the penetration depth $\Delta\lambda$ by $\Delta\lambda = -\frac{R^2}{r_s}\frac{\Delta f}{f_0}$, where R is the radius of the coil and r_s is the radius of the sample. [15] In our case, $R \sim r_s = 0.7$ mm and the reference frequency $f_0 \sim 60$ MHz such that $\Delta f = (0.16\ \mathrm{MHz}/\mu\mathrm{m})\Delta\lambda$.

The frequency shift Δf relative to the normal state and the corresponding $\Delta\lambda$ of $Sr_{0.9}La_{0.1}CuO_2$ are shown in Fig. 1a as a function of H. The inset shows the T-dependence of Δf in zero magnetic field. The normal state resonant frequency f that is reached with increasing field can only be determined for $T \geq 30$ K; for lower T the sample remains superconducting to 60 T so Δf is estimated. The frequency shift of the empty coil

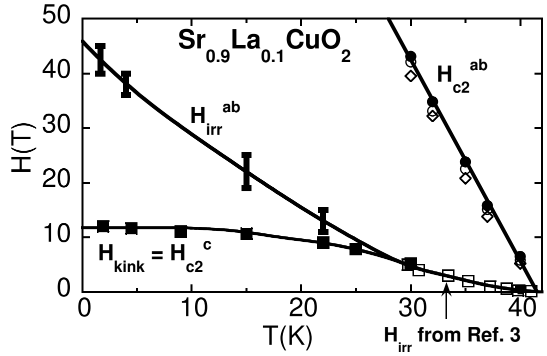

FIG. 2: Field H vs temperature T phase diagram of $Sr_{0.9}La_{0.1}CuO_2$. H_{c2}^{ab}: onset of SC where Δf exceeds 5 kHz in penetration depth measurements. Open circles and open diamonds indicate the 10 kHz and 20 kHz onsets, respectively. $H_{\rm irr}^{ab}$: onset of irreversibility in pulsed field M vs H measurements. $H_{\rm kink}$: change in slope of $\lambda(H)$, identified with H_{c2}^{c} (see text). Open squares: onset of irreversibility in M vs T measurements by Jung et al. [3] Lines are guides to the eye.

has been subtracted from all data. In applied fields, the SC transition is very broad, which can be attributed to the large anisotropy in H_{c2} of the randomly orientated grains in the polycrystal.[5] By contrast, the SC transition as a function of T at $H = 0$ is very sharp, indicating a high quality sample. Therefore, the onset of diamagnetism with decreasing H in the $\lambda(H)$ data can be identified with the largest H_{c2}, H_{c2}^{ab} for fields in the CuO_2 planes. The onset is defined as H where $\Delta f > 5$ kHz ($\Delta\lambda > 30$ nm), just above the noise of the experiment. Different onset criteria have only minor effects on the determination of H_{c2}^{ab}, as shown in Fig. 2 where H_{c2}^{ab} using an onset criteria of 10 kHz and 20 kHz are shown as open circles and diamonds, respectively. The upper critical field H_{c2}^{ab} is linear in T up to the $H = 60$ T maximum of the experiment, and extrapolates to 153 T at zero temperature. (Although if we assume the typical Werthamer-Helfand-Hohenberg curvature for an orbitally limited superconductor, [16] 153 T would constitute an upper limit for H_{c2}^{ab}). The linearly extrapolated value of 153 T is close to the s-wave Pauli paramagnetic limit of $H_{c2}^{p} = \frac{\Delta}{\sqrt{2}\mu_B} = 159$ T, where $\Delta = 13$ meV has been determined independently from STS data. [6] This raises the possibility of spin-limited superconductivity for H in the plane, which has also been observed in $YBa_2Cu_3O_{7-\delta}$.[17]

Determination of the critical fields for H along the c-axis, H_{c2}^{c}, from these data on noncrystalline samples is more difficult. However, at fields below the onset of diamagnetism we do observe a significant change in slope of the $\lambda(H)$ data, indicated as $H_{\rm kink}$ in Fig. 1b. The $H_{\rm kink}$ vs T curve is shown in Fig. 2 and extrapolates to 12 T at zero temperature. This value of $H_{\rm kink}(T = 0)$ is close to $H_{c2}^{c} = 14$ T determined from a Hao-Clem analysis mentioned previously. [5] We therefore associate $H_{\rm kink}$ with H_{c2}^{c}. In $\lambda(H)$ measurements of a noncrystalline sample, a change in slope near H_{c2}^{c} could be expected since the number of grains in the polycrystal that are superconducting varies with H for $H_{c2}^{c} < H < H_{c2}^{ab}$, whereas for $H < H_{c2}^{c}$ the entire sample is superconducting, yielding different H dependencies of the flux expulsion in these two regions. Our data yield an anisotropy ratio $\gamma = \frac{dH_{c2}^{ab}}{dT} / \frac{H_{c2}^{c}}{dT} \sim 8$, roughly in agreement with $\gamma = 9.3$ determined from low field studies. [5]

In penetration depth measurements of single crystalline organic superconductors for H along the conducting planes, a kink below H_{c2} for fields has been associated with the vortex melting transition.[15] However, in this work we have determined the vortex dynamics separately by means of magnetization measurements in pulsed fields, and we find a significant difference between the onset of irreversibility in $M(H)$, $H_{\rm irr}$, and $H_{\rm kink}$ as shown in Fig. 2. Following similar arguments for the $\lambda(H)$ measurements, we note that $H_{\rm irr}^{ab} > H_{\rm irr}^{c}$ in cuprate superconductors, therefore we assign the onset of irreversibility for polycrystalline $Sr_{0.9}La_{0.1}CuO_2$ to $H_{\rm irr}^{ab}$. Although we can't rule out the possibility that $H_{\rm kink}$ might be associated with a vortex phase transformation, the fact that $H_{\rm kink}(T \to 0)$ saturates, and $H_{\rm kink}(T \to 0) << H_{c2}^{ab}(T \to 0)$ indicates that $H_{\rm kink}(T)$ is unlikely caused by a thermally-induced vortex melting transition for $H||ab$. Future pulsed-field measurements on grain-aligned or epitaxial thin film samples will be necessary to conclusively determine whether $H_{\rm kink}(T)$ obtained in this work may be identified with $H_{c2}^{c}(T)$.

The region between $H_{\rm irr}^{ab}$ and H_{c2}^{ab} in the phase diagram in Fig. 2 is significantly larger than is observed in other electron-doped high-T_c compounds where H_{c2} typically tracks $H_{\rm irr}$. [2, 18] It is particularly surprising that $H_{\rm irr}^{ab}(T \to 0) \sim 45$ T is much smaller than $H_{c2}^{ab}(T \to 0) \sim 150$ T. In hole-doped cuprates, a large separation between $H_{\rm irr}$ and H_{c2} is often observed and is generally referred to as a vortex-liquid phase due to thermally induced fluctuations. The large discrepancy between $H_{\rm irr}^{ab}$ and H_{c2}^{ab} in e-doped $Sr_{0.9}La_{0.1}CuO_2$ even to $T \to 0$ suggests the presence of field-enhanced SC fluctuations in $Sr_{0.9}La_{0.1}CuO_2$. Enhanced SC fluctuations down to very low T may be consistent with a scenario of SC coexisting with a competing order, such as a spin-density wave (SDW) near a quantum critical point. [19] In particular, antiferromagnetic spin fluctuations associated with the competing SDW can be enhanced by external fields. [19, 20, 21] The conjecture of a competing order in the SC state of $Sr_{0.9}La_{0.1}CuO_2$ is also consistent with our recent STS studies, [22, 23] where we observe the emergence of a second energy gap with increasing tunnelling current upon the closing of the SC gap. In contrast to the SC gap, the current-induced gap is not spatially uniform probably due to interactions of the SDW with charge disorder. [21] We note that experimental evidence for coexistence of a SDW with cuprate superconductivity has been found in other high-$T_c$compounds. [24, 25, 26, 27, 28]

To further investigate the dimensionality of the superconductivity, low-field $C(T)$ and $M(T,H)$ of polycrystalline $Sr_{0.9}Gd_{0.1}CuO_2$ were measured with H up to 6 T and T down to 1.8 K in a Quantum Design Physical Properties Measurement System and a SQUID magnetometer, respectively. In contrast to in-plane Ni substitution on the Cu site, out of plane Gd substitution on the Sr site does not suppress T_c. In fact, the Gd ions exhibit local moment paramagnetism (PM) that coexists with SC to low T. [14] Figure 3 shows $M(H)$ at $T = 5$ K, and zero field/field cooled magnetization curves as a function of T in the inset. The $M(H)$ curve in the main figure can be viewed as a superposition of a SC hysteresis curve and a Brillouin function resulting from the PM of Gd. Further proof for this coexistence is evident in the inset, which shows a large positive magnetization associated with Gd paramagnetism, but nevertheless significant hysteresis between zero-field-cooled and field-cooled curves, indicating superconductivity.

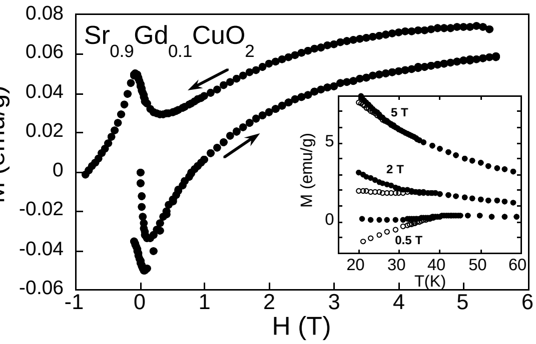

FIG. 3: Magnetization M vs H of polycrystalline $Sr_{0.9}Gd_{0.1}CuO_2$ at $T = 5$ K. Inset shows field-cooled (closed symbols) and zero-field-cooled (open symbols) M vs T data at $H = 5$ T, 2 T, and 0.5 T.

In Fig. 4, the magnitude of the paramagnetic contribution from the Gd ions is investigated quantitatively. The main figure shows $C(T)$ at $H = 0$ and $H = 6$ T. The $H = 0$ data is fit by a T^3 dependence to model the phonon contribution, (the electronic contribution at these temperature can be neglected). For $H = 6$ T, $C(T)$ can be fit by the same T^3 dependence as the $H = 0$ data, plus an additional contribution from the Gd paramagnetic moments, derived from mean field theory assuming the Hund's rule $J = 7/2$ moment, and one Gd ion for every ten unit cells. The fit is remarkable, considering that there are no fitting parameters. In the upper inset of Fig. 4, $1/\chi$ is plotted as function of T, where the line is a Curie-Weiss fit with $\mu_{\rm eff} = 8.2\mu_B$, which is close to the Hund's rule moment of 7.6 μ_B and the typically observed Gd moment of 8 μ_B. Thus we can conclude that all of the Gd ions in the sample are paramagnetic and coexist with SC down to 1.8 K, despite the close proximity of the Gd ions to the CuO_2 planes (1.7 Å). This is evidence for a strong confinement of the superconducting singlet spin pair wave function to the CuO_2 planes. On the other hand, the c-axis superconducting coherence

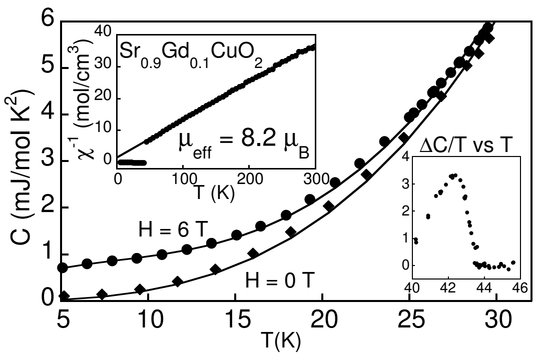

FIG. 4: Main figure: specific heat C vs T at $H = 0$ and 6 T. Lines are fits to a field-independent T^3 phonon term plus a contribution from Gd paramagetism, assuming a Gd total momentum of $J = 7/2$. Upper inset: inverse magnetic susceptibility $1/\chi$ vs T with $H = 100$ Oe, fit by a Curie-Weiss law above $T_c = 43$ K with $\mu_{\rm eff} = 8.2\mu_B$ and $\theta_{CW} = -27$ K. Lower inset: electronic specific heat ΔC vs T showing the superconducting transition.

length $\xi_c = 5.2$ Å is longer than the spacing between the Gd ion and the CuO_2 planes (1.7 Å), and also exceeds the interplane distance, implying 3D SC. The notion of 3D SC is corroborated by our STS studies, [6] which probe the charge degrees of freedom and reveal an isotropic s-wave superconducting gap. The apparent problem of 3D isotropic s-wave SC coexisting with strong Gd local moments less than 1.7 Å from the CuO_2 planes can be resolved by considering the spin and charge (orbital) degrees of freedom of the Cooper pairs separately. Whereas the singlet spin pairing is confined to the CuO_2 planes, the orbital pair wave function could still overlap adjacent CuO_2 planes, resulting in 3D SC for all values of $T < T_c$ and $H < H_{c2}$. The bulk nature of the SC is evident in the lower inset of Fig. 4, which shows the electronic contribution to C plotted as $\Delta C/T$ vs T. The peak near 43 K is associated with T_c, and the ratio $\Delta C/\gamma T_c$ is 2.9, assuming a Sommerfeld coefficient [8] of $\gamma = 1.2$ mJ/mol K^2.

In conclusion, a large upper critical field anisotropy ratio $\gamma = 8$ has been inferred from penetration depth measurements of $Sr_{0.9}La_{0.1}CuO_2$ in pulsed fields, despite the nearly cubic crystal structure. The in plane upper critical field H_{c2}^{ab} extrapolates close to the Pauli paramagnetic limit $H_{c2}^{P} = 159$ T, suggesting possible spin limiting for this orientation, as has been observed in $YBa_2Cu_3O_{7-\delta}$. [17] There is a large separation between H_{c2}^{ab} and the irreversibility field $H_{\rm irr}^{ab}$, which extends down to $T \to 0$, and is abnormal for electron doped high-T_c cuprates. This suggests the existence of field-induced superconducting spin fluctuations perhaps due to a competing SDW. In spite of the significant anisotropy in the upper critical fields, ξ_c is longer than the spacing between CuO_2 planes, indicating three-dimensionality of the orbital wave function. The low-field thermodynamic measurements of $M(T)$ and $C(T)$ for $Sr_{0.9}Gd_{0.1}CuO_2$ polycrystals indicate a coexistence of bulk SC with Gd paramagnetism, with the full $J = 7/2$ Hund's rule moment despite the close proximity of Gd atoms to the CuO_2 planes, and a T_c of 43 K in both $Sr_{0.9}Gd_{0.1}CuO_2$ and $Sr_{0.9}La_{0.1}CuO_2$. This can interpreted in terms of a strong confinement of the spin degrees of freedom of the Cooper pairs to the CuO_2 planes, whereas the orbital wave functions overlap adjacent CuO_2 planes, and exhibit isotropic s-wave symmetry as determined by STS measurements. [6]

This work was supported by the National Science Foundation under Grant No. DMR-0103045 and DMR-0405088, and the National High Magnetic Field Laboratory at Los Alamos, NM. V.Z. acknowledges support by the Caltech Millikan Postdoctoral Fellowship program.

[1] See, e.g. P. W. Anderson, "The Theory of Superconductivity in High-T_c cuprates," and references therein.
[2] M. B. Maple, E. D. Bauer, V. S. Zapf, and J. Wosnitza, 'Survey of Important Experimental Results' in "Unconventional Superconductivity in Novel Materials," Springer Verlag, to be published, and references therein.
[3] C. U. Jung *et al.*, Physica C **366**, 299 (2002).
[4] R. S. Liu *et al.*, Solid State Comm. **118**, 367 (2001).
[5] M.-S. Kim *et al.*, Phys. Rev. B **66**, 214509 (2002).
[6] C.-T. Chen *et al.*, Phys. Rev. Lett. **88**, 227002 (2002).
[7] C. U. Jung *et al.*, Phys. Rev. B **65**, 172501 (2002).
[8] Z. Y. Liu *et al.*, to appear in Europhys. Lett. (2004); available at cond-mat/0306238 (unpublished).
[9] G. V. M. Williams *et al.*, Phys. Rev. B **65**, 224520 (2002).
[10] Z. Hao *et al.*, Phys. Rev. B **43**, 2844 (1991).
[11] M.-S. Kim *et al.*, Solid State Comm. **123**, 17 (2002).
[12] D. E. Farrell *et al.*, Phys. Rev. Lett **63**, 782 (1989).
[13] D. E. Farrell *et al.*, Phys. Rev. Lett. **61**, 2805 (1988).
[14] C. U. Jung, J. Y. Kim, S.-I. Lee, and M.-S. Kim, Physica C **391**, 319 (2003).
[15] C. Mielke *et al.*, J. Phys.: Condens. Matter **13**, 8325 (2001).
[16] N. R. Werthamer, E. Helfand, and P. C. Hohenberg, Phys. Rev. B **147**, 295 (1966).
[17] J. L. OBrien *et al.*, Phys. Rev. B **61**, 1584 (2000).
[18] P. Fournier and R. L. Greene, Phys. Rev. B **68**, 094507 (2003).
[19] E. Demler, S. Sachdev, and Y. Zhang, Phys. Rev. Lett. **87**, 067202 (2001).
[20] S. Sachdev and S. C. Zhang, Science **295**, 452 (2002).
[21] C.-T. Chen and N.-C. Yeh, Phys. Rev. B **68**, 220505(R) (2003).
[22] C.-T. Chen *et al.* (unpublished).
[23] N. C. Yeh *et al.*, to appear in Physica C (2004).
[24] Y. S. Lee *et al.*, Phys. Rev. B **60**, 3643 (1999).
[25] H. J. Kang *et al.*, Nature **423**, 522 (2003).
[26] M. Matsuura *et al.*, Phys. Rev. B **68**, 144503 (2003).
[27] B. Lake *et al.*, Nature **415**, 299 (2002).
[28] H. A. Mook *et al.*, Phys. Rev. B **66**, 144513 (2002).